

# Measures for quantifying dendritic arborizations

Harry B M Uylings<sup>1,2,3</sup> and Jaap van Pelt<sup>1</sup>

<sup>1</sup> Netherlands Institute for Brain Research, Graduate School Neurosciences Amsterdam, KNAW, Meibergdreef 33, 1105 AZ Amsterdam, The Netherlands

<sup>2</sup> Department of Anatomy, Vrije Universiteit Medical Center, Amsterdam, The Netherlands

E-mail: h.uylings@nih.knaw.nl

Received 29 March 2002

Published 30 July 2002

Online at [stacks.iop.org/Network/13/397](http://stacks.iop.org/Network/13/397)

## Abstract

Topological and metrical measures are reviewed, which describe whole dendritic trees and variables within trees. These measures are applied to differentiate and classify groups of neurons. They are also of importance for simulation or reconstruction of neuronal trees in view of functional computational characteristics.

## 1. Introduction

A general feature of branching structures in nature is that they are receptive and flow-conductive. These functions can be performed optimally by branching tree structures, since they have both a relatively large interface between the branching structure and its direct environment, and a relatively shorter conductive pathway than unbranched structures would have. The shape of a neuronal tree is characteristic of the neuronal cell type. Morphometric analysis of tree structures is demanded in studies of, for instance, lifespan alterations in the dendritic/axonal field of neurons and time points of major changes; of neuronal morphological correlates of diseases; of the morphological implications of neurons under experimental conditions; and of structure–function relationships in dendritic trees. The size of neuronal trees depends upon their maturational state. Many conditions can induce changes in neuronal tree structures, such as learning, ‘enriched’ environment, hormonal fluctuations (see, e.g., Uylings *et al* (1978a, 1978b) and for recent reviews Woolley (1999), Grossman *et al* (2002)), and levels of neuronal bioelectric activity (e.g. Van Ooyen 1994, Ramakers *et al* 2001). To answer these kinds of questions, well-defined measures are needed for assessing quantitatively the morphological characteristics of neuronal branching patterns. These measures can be subdivided into those describing topological or metrical features of the whole-tree structure and those describing the local topological or metrical features within a tree, i.e. features of part of a tree. These measures can, in their turn, be used to reconstruct model tree structures for theoretical and computational purposes. In this paper we will review these topological and metrical measures.

<sup>3</sup> Author to whom any correspondence should be addressed.

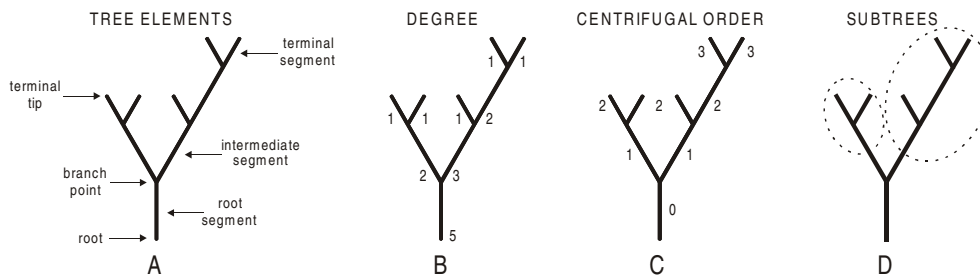


**Figure 1.** (A) Elements of a topological tree: points (root, branch point, terminal tip) and connecting segments (terminal and intermediate segments); (B) classification of segments according to the number of terminal tips peripheral to the pertinent segment, i.e. degree; (C) classification of segments according to their topological distance from the root, i.e. centrifugal order; (D) a bifurcation into two subtrees.

## 2. Neuronal structure

A neuron consists of a cell body, an axon with arborizations innervating local and remote areas, and one or more dendritic arborizations providing the receptive area for synaptic connections with innervating axons. In most morphometrical studies the number of dendritic trees per neuron is determined. In general, it is easy to establish this. However, in some neurons (e.g. reticular formation neurons or some cortical nonpyramidal neurons) it is quite difficult to determine the border between soma and the origin of a dendrite. This may affect the quantification of the number of dendrites per neuron and somatic size (see below).

## 3. Topological measures

### 3.1. 'Within-tree' variables

Topological variables ignore metrical dimensions, such as length, angle or thickness, and are only concerned with the connectivity pattern of the segments. A topological description of a neuronal tree reduces this to a *rooted* tree graph. The *root* is the origin of the dendrite or axon, generally from the neuronal cell body (figure 1).

In a topological tree one can distinguish a *root*, *branch points* and *terminal tips*, *intermediate* and *terminal segments*, and *subtrees* (figure 1(A)). In a topological analysis of tree structures (e.g. Van Pelt *et al* 1997, Van Pelt *et al* 2001a) it is informative to label segments according to the number of terminal tips ahead, i.e. *degree*: the number of tips in their peripheral subtrees with the pertinent segment as rooted segment (figure 1(B)). For grouping segments in metrical analysis or topological modelling of outgrowth, a grouping according to their topological distance from the root (i.e. *centrifugal order*) is generally applied (figure 1(C)) (Uylings *et al* 1975, Van Pelt and Verwer 1984, Van Pelt and Uylings 1999). Neuronal trees are essentially binary (e.g. Uylings *et al* 1989a), which means that branch points give rise to two subtrees. At a bifurcation the number of terminal tips is partitioned over two subtrees (figure 1(D)). The partition asymmetry index  $A_p$ , defined as

$$A_p(r, s) = \frac{|r - s|}{r + s - 2} \quad (1)$$

for  $r + s > 2$ , indicates the relative difference in the number of branch points  $r - 1$  and  $s - 1$  in both subtrees, with  $r$  and  $s$  indicating the number of terminal tips. By definition  $A_p(1, 1) = 0$ .

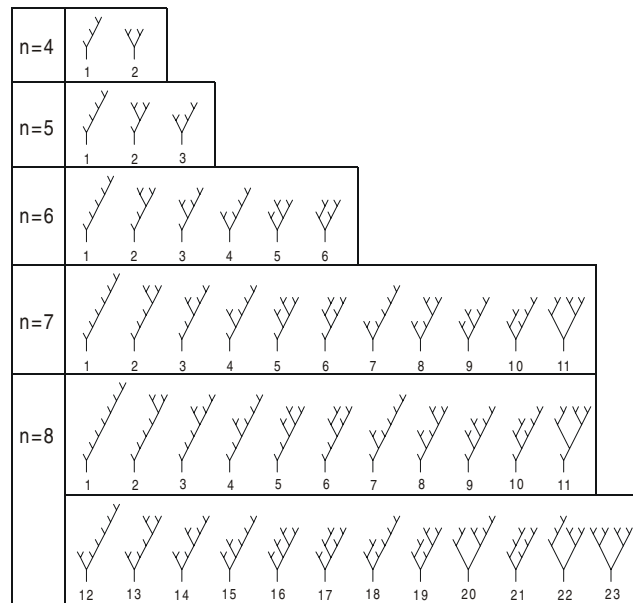


**Figure 2.** A ranking scheme of all topological tree types with 4–8 terminal tips. Modified from Van Pelt and Verwer (1984).

### 3.2. ‘Whole-tree’ topological variables

Frequently a simple variable such as *total number of segments of a tree* is applied as a means to screen for differences between different groups of neurons. Such a measure is indicative of the number of bifurcations in a tree. For a tree with only bifurcations (binary tree) with  $n$  terminal tips, the total number of tree segments  $n_s$  is

$$n_s = 2n - 1 \quad (2)$$

and the number of bifurcations  $n_p$  is

$$n_p = n - 1. \quad (3)$$

From equations (2) and (3) it follows that, for the estimation of the total number of terminal segments per tree, it is sufficient to know the number of bifurcations or terminal tips. This will reduce the effort of counting. From  $n$  or  $n_p$  the total number of segments  $n_s$  can be estimated.

*Topological tree types.* Topological trees can be distinguished by their number of segments (or branch points or terminal tips), and by the particular connectivity patterns of these segments, i.e. *topological tree types*. This provides a basis for grouping natural three-dimensional trees according to their topological tree types. From a given number of segments only a finite number of different binary rooted trees can be formed. Topological tree types can be ranked unambiguously according to their number of terminal tips and to their internal connectivity (see figure 2) using recursive rules (Van Pelt and Verwer 1983), that also allow the calculation of the exact number of 3D-topological tree types  $n_t$  (Van Pelt *et al* 1992). A reasonable approximation is given by

$$n_t \approx 2.4^n. \quad (4)$$

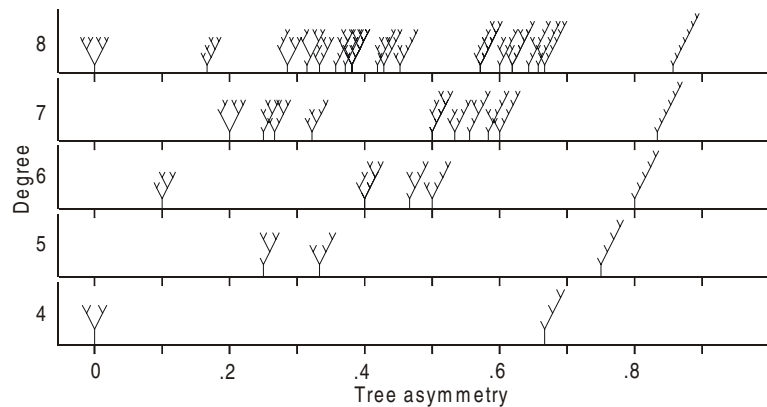


**Figure 3.** Tree asymmetry values for degree 4–8 topological tree types. The values range from 0 to the limit 1. Complete symmetrical trees have an asymmetry value of zero. Some trees with an equal asymmetry value are plotted at the same position, e.g. tree type 2 and 6 of degree 6 are plotted superimposed at the tree asymmetry value of 0.4. Modified from Van Pelt and Uylings (1999).

This step function of  $n$  shows that, although the classification according to topological 3D-tree types is the only one that uses the complete topological information of tree structures, such a classification contains an unmanageable large number of classes: e.g. for  $n = 19$ , there are 127 912 different topological tree types (see table 2 in Van Pelt *et al* 1992). For topological analysis of comparing different groups of neurons and testing different growth models, it is generally preferable to use other topological variables, containing quite a reduced number of classes (Uylings *et al* 1989a). Van Pelt *et al* (1992) developed a suitable variable for this purpose, i.e. the *tree asymmetry index*. At a bifurcation we defined the partition asymmetry,  $A_p(r, s)$ , in equation (1). The tree asymmetry of a binary tree  $A_t$  is the mean of all  $A_p$ 's. Thus

$$A_t = \frac{1}{n_p} \sum_{j=1}^{n_p} A_p(r_j, s_j) = \frac{1}{n-1} \sum_{j=1}^{n-1} A_p(r_j, s_j). \quad (5)$$

In figure 3 discrete values of the tree asymmetry for trees with  $n = 4-8$  are shown.

Although the tree asymmetry index is not able to distinguish all the tree types of the same degree (i.e. for  $n = 19$  the tree asymmetry index attains 36 904 different values among the 127 912 different tree types (Van Pelt *et al* 1992)), other measures show considerably less discriminative power (e.g. Uylings *et al* 1989a, Van Pelt *et al* 1989, 1992, Verwer *et al* 1992, Van Pelt and Uylings 1999). For testing growth models and detecting differences between groups of neuronal trees, sufficient characteristic topological information has been kept to be discriminative. The expected value of the tree asymmetry index for a set of trees appears to be strongly related to the mode of growth, and appears to be rather insensitive to the degrees of the trees. This has the advantage that a set of trees with different degrees can be characterized by one single number (the mean tree asymmetry), irrespective of the sizes of the trees (Van Pelt *et al* 1992). When a set of trees consists of both very small ( $n < 10$ ) and large ( $n > 10$ ) ones, the variance in the mean tree asymmetry will be dominated by the group of small trees. It is then advisable to divide the data sets in two tree size classes (e.g.  $n < 10$  and  $n > 10$ ) and to test per size class (Van Pelt *et al* 1992).

In the past other topological measures have been used for topological characterization of trees. Sadler and Berry (1983, 1988) proposed the 'vertex ratio' and the 'terminal/link ratio'. The vertex ratio is the ratio of the number of subtrees of degree 2 ( $T(2)$ ) and the degree

of the whole tree minus twice the number of degree 2 subtrees ( $n - 2T(2)$ ), Verwer *et al* (1992). The amount of information contained in the vertex ratio is rather low as measured by its value domain (Uylings *et al* 1989a). The vertex ratio has been applied by Sadler and Berry (1983, 1988) in growth analyses of Purkinje cell dendritic fields, which are very large trees. It is applicable for large, strictly binary trees. For trees with a significant number of trifurcations the ‘terminal/link ratio’ was developed. Horsfield and Woldenberg (1986) show that the information of the vertex ratio is comparable with that of the branching ratio of Strahler orders. They prefer the branching ratio, when trees have been pruned. The ‘terminal/link ratio’ is the number of terminal segments,  $n_t$ , divided by the total number of segments,  $n_s$ , at *each* centrifugal order, figure 1 (Verwer *et al* 1992). A similar measure, i.e. ‘1 minus terminal/link ratio’ for each centrifugal order was developed earlier by Smit *et al* (1972). We have abandoned this measure and strongly prefer nowadays *the tree asymmetry index*. This index is also suitable for relatively small trees, and very suitable for mathematical growth model testing, as indicated above and in Van Pelt and Uylings (2002).

#### 4. Metrical measures

An important aspect, in fact for all metrical variables, is the influence of deformation (shrinkage) due to the histology. We have to keep aware of these influences and to determine the effect (where possible) (e.g. Uylings *et al* 1986a).

##### 4.1. Somatic size

In many morphometrical studies somatic size is estimated for a first characterization. The somatic surface area is one of the variables of importance for electrophysiological modelling (e.g. Rall 1977). Due to the optical shadow of somata, which are tracer-filled or Golgi-impregnated, somatic depth measurements are generally inaccurate. For practical reasons, the somatic size is estimated from its projected area or cross-sectional area (e.g. Uylings *et al* 1986b). Somatic size is also, but less frequently, estimated by its projected surface area  $S_p$ , or volume  $V$ , of a prolate spheroid on the basis of the length of the major and minor axes,  $A$  and  $B$ , respectively, of the projected soma, using the following equations:

$$S_p = (\pi/4)AB \quad (6)$$

$$V = (\pi/6)AB^2 \quad (7)$$

where  $A$  is the major axis, i.e. the longest axis of the soma, and  $B$  is the length of the minor axis, i.e. the longest axis perpendicular to the major axis. The projected somatic surface area of, for example, cortical pyramidal and nonpyramidal cells, Purkinje neurons, motoneurons and retinal ganglion cells is frequently reported to be moderately, but significantly, correlated with the total dendritic length (e.g. Hillman 1979, McMullen *et al* 1984, Jin *et al* 2001). As mentioned above, the border between soma and the origin of a dendrite can be ambiguous in some neurons (Leontovich 1973). The estimation of soma size and number of dendrites per cell is consequently more difficult, the more so when the root segment (figure 1) bifurcates after a small distance. In such a situation the following criteria are useful. Dendrites have a much smaller diameter than soma. A dendritic base is relatively thick in comparison to its root segment, but this base tapers relatively fast. Usually a large part of the dendritic base is considered to be part of the soma, when the extrapolated somatic outline passes through the base. This outline passes through the ‘origin’ of a dendrite. Somatic size appears to change significantly under particular experimental conditions (e.g. Headon *et al* 1979, Rauschecker 1997) and during developmental stages (e.g. Uylings *et al* 1994).

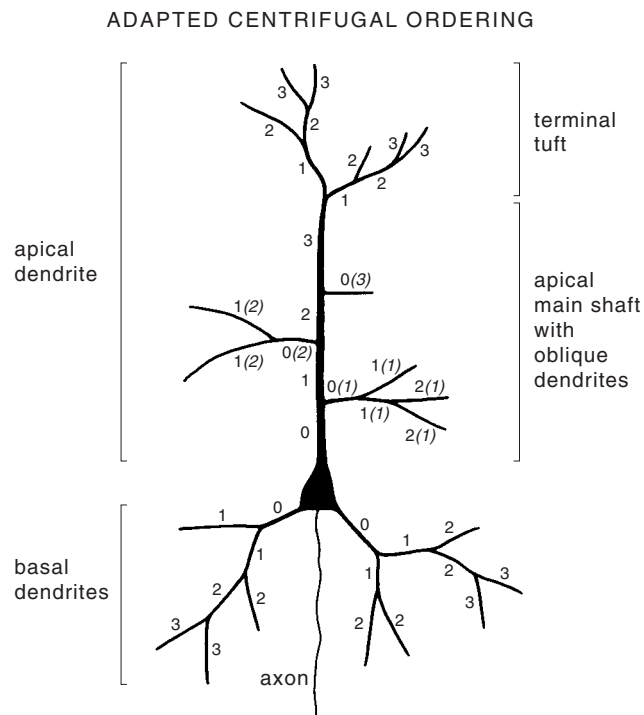


**Figure 4.** Centrifugal ordering for basal dendrites of pyramidal neurons. The centrifugal ordering has been adapted for apical dendrites. To avoid assigning equal orders to different kinds of dendritic segments, the apical dendrite is divided into a main shaft with a terminal tuft and oblique dendrites (from Uylings *et al* (1986b)).

#### 4.2. 'Within-tree' variables

Metrical variables for a segment are *segment length*, *diameter* and *membrane area*. These variables are also of importance for electrophysiological characteristics of the dendrite (e.g. Rall 1977, Horwitz 1981). The diameter can taper significantly along a segment and then it has to be estimated at different places along the pertinent segment. *Diameter* measurements are meaningful when the diameter values are not close to the resolving power of the microscope (i.e. about  $0.5 \mu\text{m}$ ). From studies on *segment length* (reviewed by Uylings *et al* 1986b, 1989b) it appears to be essential to distinguish different groups. A first distinction that is essential for nearly all neuronal types is between *terminal* and *intermediate* segments (see table 2 in Uylings *et al* (1986b)). Such a subdivision enabled us to detect changes in the length in dendritic terminal segments in adulthood due to a so-called enriched environment Uylings *et al* (1978a, 1978b). For cortical neurons it appeared to be important to group terminal segments according to centrifugal order (figure 4; e.g. Uylings *et al* 1978a, 1994). The lower the centrifugal order, the higher the mean terminal segment length value.

For intermediate segments a subgrouping appears to be necessary as well. So far only cortical pyramidal, nonpyramidal and dentate granule neurons have been studied for this aspect. There it appears to be essential to distinguish intermediate segments according to the degree of their peripheral subtree (figure 5), but not versus centrifugal order (Uylings *et al* 1986b, 1989b, 1994). The largest mean length value for intermediate segments have been found for the most peripheral intermediate segments, those with degree 2.

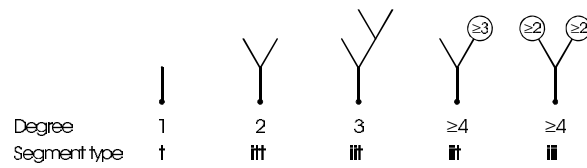


**Figure 5.** Segment classification according to degree and segment type. (t): terminal segments, (itt): intermediate segment bifurcating into two terminal segments, (iit): intermediate segment bifurcating into an intermediate and terminal segment, (iii): intermediate segment bifurcating into two intermediate segments. Modified from Uylings *et al* (1986b).

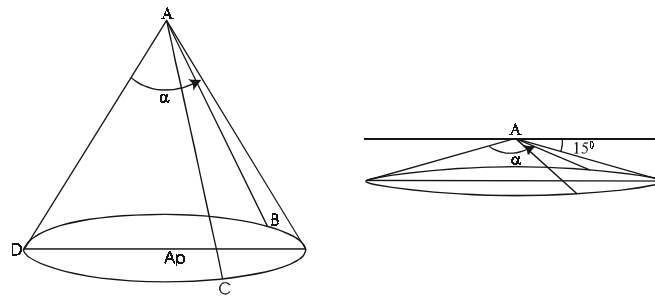


**Figure 6.** Bifurcation with segments DA, AB and AC wrapped by a cone. The cone angle,  $\alpha$ , defines the flatness of a bifurcation. Flat bifurcations have an  $\alpha = 180^\circ$ ; in the right panel  $\alpha = 165^\circ$ .  $A_p$  is the projection from A on plane DBC.

*Bifurcation angles* have been determined in relatively few studies. Bifurcation angles are useful for spatial reconstructions and display unimodal distributions (Mungai 1967, Smit and Uylings 1975, Wolf *et al* 1995). These distributions, however, display a very large variability and quite wide modal values (e.g. Smit and Uylings 1975, Wolf *et al* 1995). In addition, the angle values did not show significant alterations in ageing or senile dementia (Williams and Matthijsse 1986) and after exposure to a so-called enriched condition (Uylings *et al* 1978a). On the other hand, the dendritic bifurcations have their parent and daughter segments mainly located in or near a flat plane (Uylings and Smit 1975). This has been determined in the following way: consider a bifurcation with a parent segment and two daughter segments as a bifurcation pyramid. Enwrap this pyramid by a ‘right circular cone’ (figure 6) and the cone angle  $\alpha$  specifies the flatness of a bifurcation, i.e. maximum values for maximum flatness.

Bifurcations lying in a flat plane have a cone angle  $\alpha$  of  $180^\circ$ , and the larger the deviation from a plane, the smaller the cone angle (figure 6). The value of the cone angle  $\alpha$  is related to the bifurcation angles according to equation (8):

$$0.5(1 - \cos \alpha) = \frac{4x^2y^2z^2}{4x^2y^2 - (x^2 + y^2 - z^2)^2} \quad (8)$$

(Uylings and Veltman 1975), in which  $x = \sin \frac{1}{2}\rho$ ,  $y = \sin \frac{1}{2}\sigma$  and  $z = \sin \frac{1}{2}\tau$  with  $\rho = \angle BAC$  (figure 6) is the intermediate angle,  $\sigma = \angle DAB$  (side angle) and  $\tau = \angle DAC$  (side angle). The cone angle  $\alpha$  relates to the dimensionless solid angle  $\Omega$  as

$$\Omega = 2\pi(1 - \cos \frac{1}{2}\alpha). \quad (9)$$

The solid angle is a measure for 3D space contained in a conical sector of a sphere. From equation (9) it follows that the solid angle reaches its maximum value when the bifurcation lies in a flat plane:  $\Omega = 2\pi$ . For the aspect of flatness of a bifurcation or the deviation from a

plane, we prefer the variable cone angle  $\alpha$  above the solid angle  $\Omega$ . The cone angle is linear, proportional to the plane deviation, while the solid angle is proportional via a cosine function. The distribution of the cone angle  $\alpha$  is a sharp unimodal one (Uylings and Smit 1975) and shows that the large majority of bifurcations have their segments in or close to a flat plane. Such a finding is expected when, during development, the outgrowing neurites exert elastic tensions on the dendritic structure (Dennerl *et al* 1988, Van Veen and van Pelt 1992) and forced equilibria cause the parent and daughter segments at a bifurcation to be aligned as much as possible in a flat plane. A planar arrangement of segments is also predicted for optimal flow across a bifurcation. When bifurcations have their segments in or close to a flat plane, the next angular measure, i.e. the angle between consecutive bifurcations, might be of interest. In basal dendrites of pyramidal cells we only found a flat distribution, indicating no preferential orientation of bifurcation planes (Uylings and Smit 1975). A preferential orientation exists for the bifurcation planes in, for example, Purkinje cells.

#### 4.3. 'Whole-tree' variables

The simplest 'whole-tree' metrical variable frequently applied in morphometrical studies is the total length of all dendritic segments per cell, i.e. *total dendritic length* per cell. This variable showed the existence of general size differences between groups of neurons (e.g. Uylings *et al* 2000) and the differential rate of growth in developmental studies (e.g. Koenderink *et al* 1994, Koenderink and Uylings 1995, Uylings *et al* 1994). However, the total dendritic length variable is susceptible to cutting when it is determined in single histological sections (Uylings *et al* 1989b). When the dendritic field has a strong preferential orientation in 3D space (e.g. Leontovich 1973, Fiala and Harris 1999), this effect can be dramatic when the plane of cutting does not account for this preferential orientation. In general, more than 75% of the 'total dendritic length' per cell is formed by the total length of all individual *terminal* segments (Uylings *et al* 1989b). The effect of cutting on the variable *total dendritic length per neuron* can be reduced by comparing the pattern of differences in lengths of individual terminal segments only between different groups of subjects. Then the assumption is that the sample of uncut terminal segments in the thick single section is representative of the length of all terminal segments. This is a reasonable one, when a preferential orientation of the dendritic tree is accounted for. Additional 'whole-tree' variables are '*path length*' from terminal tip along segments to the dendritic origin (e.g. Van der Loos 1959) and '*radial distance*' from terminal tips to dendritic origin (e.g. De Ruiter and Uylings 1987). Differences between path length and radial distance indicate the 'straightness' of neuronal branches (De Ruiter and Uylings 1987, Cannon *et al* 1999).

#### 4.4. Orientation of whole trees

For the estimation of the spatial extent of 'whole' trees, the so-called Sholl's analysis is still the most frequently used. In Sholl's analysis (1953) a set of equidistant concentric spheres, or, in its projection variant (Eayrs 1955), a set of two-dimensional concentric circles, is used and the number of intersections is counted with equidistant consecutive spheres and circles, respectively, with the soma as the centre.

The two-dimensional variant with the set of concentric circles is similar to a set of concentric cylinders in 3D. The popularity of this method is probably due to the fact that it is easy and because it allows detection of differences between groups of neurons when these differences are very large. However, it is not a sensitive method, since it can assign the same series of intersection numbers to a set of concentric spheres for different types of trees. Also,

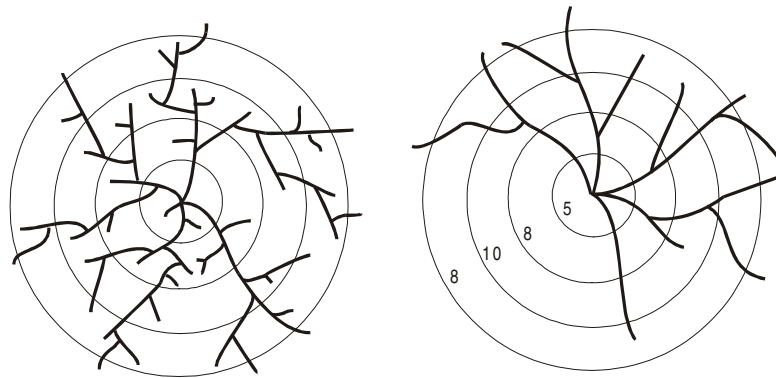


**Figure 7.** This schematic figure shows that the Sholl measure of the series of numbers of intersections with concentric spheres/circles can be identical for trees, which have different topological and metrical features. The series of numbers of intersections in both the left and right panel is 5, 8, 10 and 8, respectively. In addition, tree orientation differences will not be detected with this measure. The left panel is modified from MacDonald (1983).

this method does not distinguish orientation differences (Uylings *et al* 1989a, 1989b), see figure 7. A well-known example is the study of Valverde (1970), in which Sholl's method did not reveal a difference, whereas Ruiz-Marcos and Valverde (1970), examining the same groups of neurons, detected significant differences in dendritic orientation. A similar, more recent, example is the study by Kossel *et al* (1995). The concentric-circle method can be improved by dividing the circles into different sectors of, e.g.,  $30^\circ$  (see, e.g. Uylings *et al* (1989b)).

However, this is only appropriate for 2D structures. The approach of O'Hanlon and Lowrie (1996), who applied the 2D equiangular sector division in two orthogonal planes, is interesting. However, the thicker the sections, the more the procedure turns into an analysis of 3D space, which means 3D-space sectors have to be taken into account (see below). At first glance the subdivision of the concentric spheres of Sholl's analysis into sectors with equal conical angles (e.g. McMullen *et al* (1984, 1988) used equidistant cone angular intervals of  $15^\circ$  and  $30^\circ$ ) seems to be allowed. However, the relationship given in equation (9) for the solid angle, which is a measure for 3D space contained in a cone, shows that it is not. Equation (9) specifies that the 3D spaces contained in the conical sectors of a sphere with equidistant cone angles are not identical. This is illustrated in figure 8 for equidistant intervals of  $30^\circ$ . The space of conical sector I (lower panel of figure 8) is then less than one-third of the space between cone II and the mid-plane of conical sector III. The latter space is  $\pi$  sr (lower panel of figure 8).

To obtain six spherical sectors with equal space volumes, it follows from equation (9) that we need cones with  $\frac{1}{2}\alpha$  values of  $48.2^\circ$ ,  $70.5^\circ$  and  $90^\circ$ , respectively. This is displayed in the upper panel of figure 8. The interesting 'fan-in' display method of Glaser and McMullen (1984) can be subdivided into equispatial sectors, as is shown in figure 8, derived from equation (9), but dividing the space into equiangular sectors does not result in equal solid angles. See Uylings *et al* (1989b) for a further detailed description.

Another popular method for orientation analysis is the *principal axes method*. For (projected) 2D neuronal tree analysis the principal axis method was introduced by Colonnier (1964). He defined the major axis geometrically as the maximum distance between two terminal tips along the soma and the minor axis as the maximum distance between terminal tips perpendicular to the major axis. Stevens and Van den Pol (1982) defined these two axes mathematically. For each midpoint of a dendritic segment they defined a mass-weight

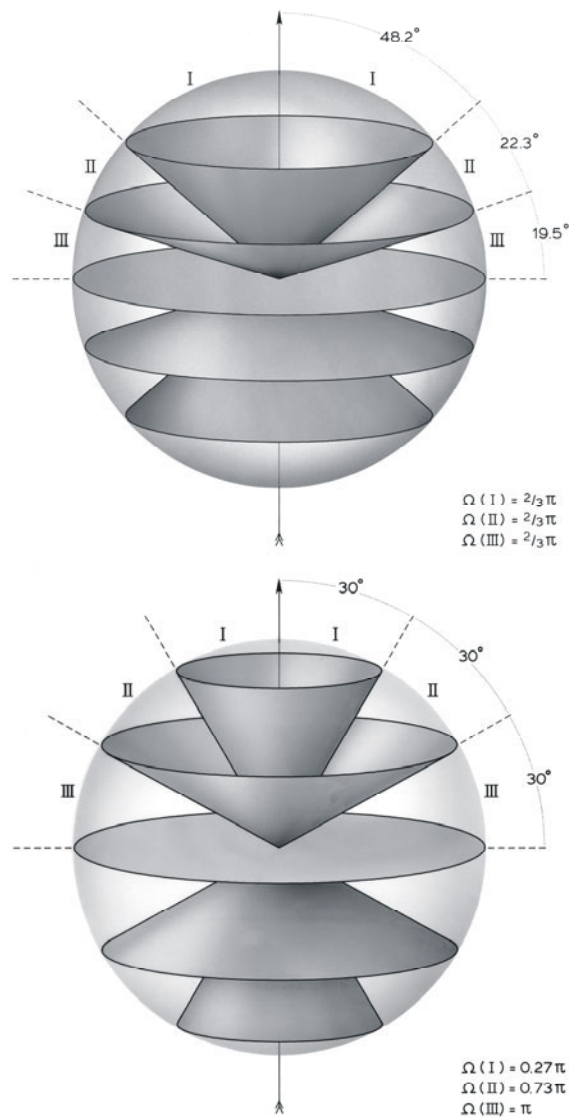


**Figure 8.** Division of spherical space into sectors with identical space (upper panel) results into cone angles of these sectors I, II and III with different values, i.e.  $(2\alpha)$  is  $48.2^\circ$ ,  $22.3^\circ$  and  $19.5^\circ$ , respectively. When these cone angles are identical, the spherical space ( $\Omega$ ) in these sectors is different (lower panel). From Uylings *et al* (1989b).

which is proportional to the length of the pertinent segment (figure 9). With these mass-weighted midpoints the ‘centre of mass’ (i.e. the centroid) for the whole 2D dendritic field was determined, on the basis of which the major and minor axes were defined (see figure 9). The major axis is the rotational axis with the smallest moment of inertia, and the minor axis is perpendicular to the major axis through the centroid.

This method was used by, for example, Borges and Berry (1978) to study Purkinje cell dendritic fields and Leventhal and Schall (1983) and Schall and Leventhal (1987) to study

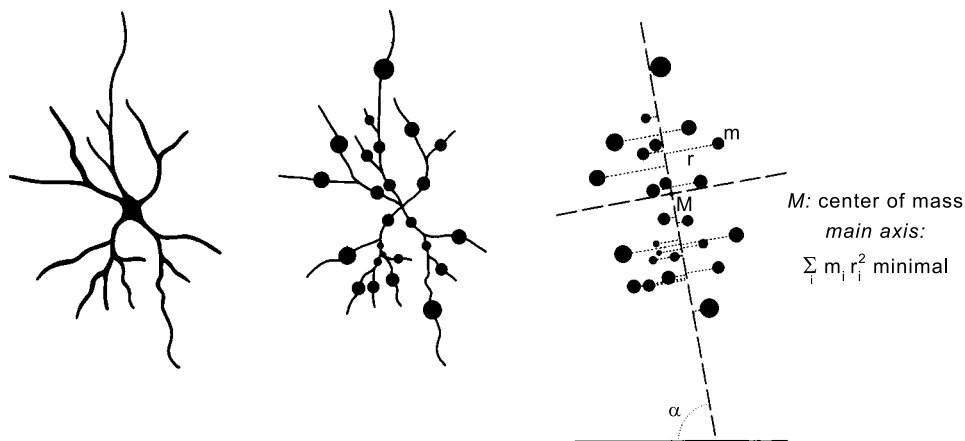


**Figure 9.** Principal component axes of a 2D neuronal field, i.e. the first (major) axis and the second (minor) axis. Left panel: a 2D neuron (adapted from Colonnier (1964)). Middle panel: the relative size of the black dots specifies the relative weight of the mass of the different segments. The weight is proportional with segment length. The right panel illustrates the calculation of the major and minor (perpendicular to major) axes.

retinal ganglion cells. This 2D principal axis method was extended to a 3D principal component analysis (PCA) by Brown (1977) and later applied by, for example, Yelnik *et al* (1983) and Fénelon *et al* (1994). For a detailed description see the review by Uylings *et al* (1989b). In general, this 3D principal component method is an appropriate method for 3D tree structures, when the whole 3D dendritic field has been reconstructed. However, a few 3D dendritic fields display a curvilinear orientation in all directions; for example, dendritic fields of primate substantia nigra neurons (Francois *et al* 1987), in which case this principal component method is not the optimal method (e.g. Francois *et al* (1987)).

When the whole 3D tree structure is not completely constructed, a sensible approach to detect a preferential orientation of the tree structure is to study neurons in sections cut in different planes (e.g. coronal, sagittal and horizontal). In this way Parnavelas and Uylings (1980) detected a preferential orientation in cortical multipolar nonpyramidal cells towards the pial membrane and the white matter. This was later confirmed by Jin *et al* (2001) with a vector analysis method.

Another interesting method for the detection of a preferential orientation in the dendritic field is the *Cartesian grid analysis* method developed by Ruiz-Marcos (1983). In the 2D version of this method the whole dendritic field is projected onto a 2D Cartesian grid of square elements equal to  $15 \times 15 \mu\text{m}^2$ . In each square (in each voxel in the 3D version) the dendritic length is determined for each neuron. The orientation of groups of neurons can then be statistically compared with this method (e.g. Ruiz-Marcos and Ipiña 1986, Uylings *et al* 1986b, 1989b, 1994).

## 5. Metrical tree variables estimated by stereological principles

Stereological principles are applied to estimate 3D quantities (such as volume, total number of cells, etc) from sections through the object of interest (e.g. Howard and Reed 1998). In the last decade, stereological principles were developed (e.g. Gokhale 1990, Cruz-Orive and Howard 1991) to estimate the length of 3D branching structures using total vertical projections.

'Vertical projections' are the projections on a set of systematic random planes around a vertical axis in the 3D slice. This can be easily applied to 3D neuronal tree analysis when confocal microscopy is available and an isolated neuron with dendrites is completely contained in a very thick section. Such a neuron can be recorded in a set of confocal sections, after which the projection upon a set of about 3–6 systematic random planes around a vertical axis can be obtained. The total length of the neuron can then be estimated by counting the number of intersections ( $I$ ) with a cycloid test grid, according to the following equation (Cruz-Orive and Howard 1991, Howard *et al* 1992):

$$\text{est}\{L(\text{tree})\} = 2 \frac{a}{lM} \text{mean}(I) \quad (10)$$

where  $a/l$  is the  $\text{cm}^2$  plane area per 1 cm cycloid arc,  $M$  is the linear magnification and  $\text{mean}(I)$  is the total number of intersections of projected dendrites with the superimposed cycloid test grid divided by the number of vertical projection planes studied. The  $\text{est}\{L(\text{tree})\}$  is an unbiased estimate, but its variance will depend on the orientation of the vertical axis (Roberts and Cruz-Orive 1993). When a group of neurons with dendrites is stained and contained in a 3D slice, the mean dendritic length per neuron can be estimated by

$$\text{est}\{\bar{L}_n\} = \frac{\text{est}\{L(\text{trees})\}}{N_v} \quad (11)$$

where  $\text{est}\{L(\text{trees})\}$  is the total dendritic length of the neurons and  $N_v$  is the total number of neurons contained in the 3D slice studied. The above-mentioned estimates of  $\text{est}\{L(\text{tree})\}$  and  $\text{est}\{\bar{L}_n\}$  can be performed in a relatively short time, when all the trees are scanned by a confocal microscope. For more detailed questions about the length of individual segments of a particular order and/or degree (figure 5), it is necessary to assign a correct order and degree to segments. A manual labelling of order number and degree number is, however, very tedious and time-consuming and software programs are required that are applicable to completely reconstruct trees. On the other hand, when whole trees are scanned, the dendritic lengths can be determined with special software programs like those developed by Pool (Ramakers *et al* 2001).

Roberts and Cruz-Orive (1993) further developed this type of stereological analysis so that it is possible to estimate the dendritic length contained in a spherical 3D space contained between two concentric cones (e.g. figure 8; their figure 2). For this stereological analysis it is, however, necessary to ascertain first of all in which spherical sector between cones parts of the tree are located. This can be done with software packages. Then the intersections of dendritic projections can be manually counted with a cycloid grid in systematic random vertical planes that are subdivided into spatial compartments (see equation (9) above and the section on 'orientation of whole trees'). In contrast to cycloid intersection counting, an automatic estimation of the above-mentioned dendritic length in these spatial sectors from voxel data is biased and non-trivial according to Roberts and Cruz-Orive (1993) and Dorst and Smeulders (1987).

Until now, the above-mentioned stereological approaches have seldom been applied in neurobiology, but we mention them here for their attractive concepts.

## 6. Fractal analysis of trees

Fractal characteristics of dendritic trees relate to geometrical properties at various spatial resolutions. Although log–log plots of these relations generally show multiple gradients, indicating the lack of a single fractal dimension, these plots may still bear meaningful geometrical characteristics of dendritic branching patterns (Cannon *et al* 1999, Costa *et al* 2002).

## 7. Analysis of spines on dendrites

Axons have specialized contacts (synapses) on dendritic shafts, but most central excitatory synapses are on small dendritic protrusions, i.e. spines (e.g. Shepherd 1996, Andersen and Figenschou Soleng 1999). Interesting reviews of the different shapes of spines on different types of neurons are those by Fiala and Harris (1999) and Harris and Kater (1994). The quantitative analysis of the spine density along dendrites is of importance to demonstrate the first noticeable morphological alterations due to hormonal fluctuations or environmental or learning conditions (see for a review, e.g., Woolley 1999) and is also important for computational aspects of electric activity distribution over dendritic trees (e.g. Segev *et al* 1995, Shepherd 1996). However, quantitative analysis of spines is quite difficult, not only because of their small dimensions, but also because of the heterogeneity of spine densities within the dendritic tree and between trees (for cortical pyramidal neurons see, for example, Ruiz-Marcos *et al* (1988) and for CA1 neurons see, for example, Fiala and Harris (1999)). Due to their small dimensions spines can be obscured in light microscopy by dendritic shafts. Very often it will be necessary to correct quantitatively for the hidden spines, which depends upon spine length and dendritic diameter (Feldman and Peters 1979, Bannister and Larkman 1995, Trommald *et al* 1995) or to obtain 3D reconstructions of dendrites with their spines (White and Rock 1980, Harris and Stevens 1989, Belichenko and Dählström 1995). It is therefore a relief when the effects on spine density are so dramatic that no quantitative analysis is necessary (e.g. Woolley 1999). Also, when the dendritic diameter becomes smaller through, for example, ageing, no correction factors are necessary for questions about whether or not different conditions lead to a spine loss (e.g. De Ruiter and Uylings 1987). A good quantitative analysis, however, remains a requisite for those studies that are related to neuronal computation (e.g. Fiala and Harris 1999).

## 8. A multivariable description and multivariate statistical analysis

In the previous sections we reviewed quite a number of measures that describe different aspects of tree structures. In general, groups of neurons are statistically compared for single variables. Multivariate statistical comparison is, however, essential when different neuronal cell types are compared, with the question: do they differ significantly and, if they do, for which features? To be able to answer these questions, multidimensional scaling (MDS) and hierarchical cluster analysis (HCA) are applied (e.g. Kötter *et al* 2001) to detect and distinguish 'natural groupings' in a set of different cell groups by measuring 'similarity' or 'dissimilarity' (e.g. Chatfield and Collins 1980, Everitt and Dunn 1992). The multivariate PCA has also been applied to find an answer to the above-mentioned questions (e.g. Pearson *et al* 1985, Fénelon *et al* 1994). This type of analysis transforms a set of observed variables to a new set of variables, which are uncorrelated and arranged in a decreasing order of variance (Chatfield and Collins 1980). The first principal component accounts for as much variation in the original data as possible. Cannon *et al* (1999) applied a PCA using a battery of 32 morphometrical, topological and fractal parameters to investigate neuronal groupings and growth characteristics in different sets of hippocampal neurons. They concluded that the PCA combined measures had only slightly greater discriminative power than the best individual measures, comprising the number of branch points and total length and area. For this type of analysis they used data of CA1 pyramidal cells from Turner available in a worldwide database (Cannon *et al* 1998).

The above-mentioned multivariate methods are descriptive. An analytical method to test the existence of differences among the means of several cell groups is the canonical variate analysis (CVA) (Chatfield and Collins 1980). The CVA is invariant when the origin and scale of

measurements are different, unlike the PCA. CVA assumes, however, normal distributions and homogeneity of the variance–covariance matrices. Ipiña and Ruiz-Marcos (1986) and Ipiña *et al* (1987) showed, with CVA, that hypothyroidism affects both basal and apical dendrites and that tyrosine replacement therapy did not improve the effects. Another approach to detect statistical difference is the application of Hotelling's *T* square test using the Mahalanobis distance between vectors of two multivariate distributions (Schleicher *et al* 2000, Bartels 1981). For approaches with multivariate analysis the availability of databases is instrumental (Van Pelt *et al* 2001b).

## 9. Summary and discussion

This paper has reviewed several measures for the quantification of neuronal shapes. A distinction has been made between topological and metrical variables, and between within-tree and whole-tree variables. The measures used for geometric quantification of dendritic arborizations are, however, usually applied to their reconstructions, and seldom to the structures themselves. Dendritic reconstructions result in geometric approximations of the original object, dependent on the reconstruction approach used. The usual manual approach approximates dendritic branching patterns by a set of connected regular cylindrical objects, allowing quantification in terms of the measures reviewed in this paper. These geometrical details form the basis for the characterization of cell groups (for instance using multivariate approaches), but, reciprocally, their experimental distributional properties can also be used to synthesize dendritic trees with similar statistical geometrical properties. For instance, Ascoli (2002) describes stochastic algorithms for synthesizing neuronal shapes on the basis of segment diameters and distances from the soma. Segmentation of neuronal objects from confocal digitized images preserve much of the geometrical details. These developments in image analysis will also stimulate the development of other classes of shape parameters (Costa *et al* 2002), and possibly also dendritic modelling approaches towards improved morphological details. These developments will also stimulate studies of the functional implications of dendritic shape. For instance, Van Ooyen *et al* (2002) made it clear that dendritic topology can influence the spiking behaviour of neurons, and emphasize the impact of metrical properties on neuronal firing as shown by other investigators.

## Acknowledgments

The authors thank Ms W T P Verweij for her secretarial assistance in the preparation of this paper and Mr H Stoffels and Mr G van der Meulen for their drawings and photographs, respectively.

## References

- Andersen P and Figenschou Soleng A 1999 A thorny question: how does activity maintain dendritic spines? *Nat. Neurosci.* **2** 5–7
- Ascoli G 2002 Neuroanatomical algorithms for dendritic modelling *Network: Comput. Neural Syst.* **13** 247–60 (this issue)
- Bannister N J and Larkman A U 1995 Dendritic morphology of CA1 pyramidal neurones from the rat hippocampus: II. Spine distributions *J. Comp. Neurol.* **360** 161–71
- Bartels P H 1981 Numerical evaluation of cytological data. VII. Multivariate significance tests *Anal. Quant. Cytol.* **3** 1–8
- Belichenko P V and Dählström A 1995 Studies on the 3-dimensional architecture of dendritic spines and varicosities in human cortex by confocal laser scanning microscopy and Lucifer yellow microinjections *J. Neurosci. Methods* **57** 55–61

- Borges S and Berry M 1978 The effects of dark rearing on the development of the visual cortex of the rat *J. Comp. Neurol.* **180** 277–300
- Brown C 1977 Neuron orientations: a computer application *Computer Analysis of Neuronal Structures* ed R D Lindsay (New York: Plenum) pp 177–88
- Cannon R C, Turner D A, Pyapali G K and Wheal H V 1998 An on-line archive of reconstructed hippocampal neurons *J. Neurosci. Methods* **84** 49–54
- Cannon R C, Wheal H V and Turner D A 1999 Dendrites of classes of hippocampal neurons differ in structural complexity and branching patterns *J. Comp. Neurol.* **413** 619–33
- Chatfield C and Collins A J 1980 *Introduction to Multivariate Analysis* (London: Chapman and Hall) p 246
- Colonnier M 1964 The tangential organization of the visual cortex *J. Anat.* **98** 327–44
- Costa L F, Manoel E T M, Faucereau F, Chelly J, Van Pelt J and Ramakers G J A 2002 A multiscale framework for neuromorphometry *Network: Comput. Neural Syst.* **13** 283–310 (this issue)
- Cruz-Orive L M and Howard C V 1991 Estimating the length of a bounded curve in 3D using total vertical projections *J. Microsc.* **163** 101–13
- Dennerl T J, Joshi H C, Steel V L, Buxbaum R E and Heidemann S R 1988 Tension and compression in the cytoskeleton of PC12 neurites: I. Quantitative measurements *J. Cell Biol.* **107** 665–74
- De Ruiter J P and Uylings H B M 1987 Morphometric and dendritic analysis of fascia dentata granule cells in human ageing and senile dementia *Brain Res.* **40** 217–29
- Dorst L and Smeulders A W M 1987 Length estimations for digitized contours *Comput. Vis. Graph. Image Process.* **40** 311–33
- Everys J T 1955 The cerebral cortex of normal and hypothyroid rats *Acta Anat.* **25** 160–83
- Everitt B S and Dunn G 1992 *Applied Multivariate Data Analysis* (New York: Oxford University Press) p 304
- Feldman M L and Peters A 1979 A technique for estimating total spine numbers on Golgi-impregnated dendrites *J. Comp. Neurol.* **188** 527–42
- Fénelon G, Yelnik J, François C and Percheron G 1994 Central complex of the primate thalamus: a quantitative analysis of neuronal morphology *J. Comp. Neurol.* **342** 463–79
- Fiala J C and Harris K M 1999 Dendritic structure *Dendrites* ed G Stewart, N Pruston and M Häusser (New York: Oxford University Press) pp 1–34
- Francois C, Yelnik J and Percheron G 1987 Golgi study of the primate substantia nigra. II. Spatial organization of dendritic arborizations in relation to the cytoarchitectonic boundaries and to the striatonigral bundle *J. Comp. Neurol.* **265** 473–93
- Glaser E M and McMullen N T 1984 The fan-in projection method for analyzing dendrite and axon systems *J. Neurosci. Methods* **12** 37–42
- Gokhale A M 1990 Unbiased estimation of curve length in 3D using vertical slices *J. Microsc.* **159** 133–41
- Grossman A W, Churchill J D, Kleim J A, Bates K E and Greenough W T 2002 A brain adaptation view of plasticity: is synaptic plasticity an overly limited concept? *Prog. Brain Res.* at press
- Harris K M and Kater S B 1994 Dendritic spines: cellular specializations imparting both stability and flexibility to synaptic function *Annu. Rev. Neurosci.* **17** 341–71
- Harris K M and Stevens J K 1989 Dendritic spines of CA1 pyramidal cells in the rat hippocampus: serial electron microscopy with reference to their biophysical characteristics *J. Neurosci.* **9** 2982–97
- Headon M P, Sloper J J, Hiorns R W and Powell T P 1979 Cell size changes in undeprived laminae of monkey lateral geniculate nucleus after monocular closure *Nature* **281** 572–4
- Hillman D E 1979 Neuronal shape parameters and substructures as a basis of neuronal form *The Neuroscience Fourth Study Program* ed F O Schmitt and F G Worden (Cambridge, MA: MIT Press) pp 477–98
- Horsfield K and Woldenberg M J 1986 Comparison of vertex analysis and branching ratio in the study of trees *Respir. Physiol.* **65** 245–56
- Horwitz B 1981 Neuronal plasticity: how changes in dendritic architecture can affect the spread of postsynaptic potentials *Brain Res.* **224** 412–18
- Howard CV, Cruz-Orive L M and Yaegashi H 1992 Estimating neuron dendritic length in 3D from total vertical projections and from vertical slices *Acta Neurol. Scand.* **137** 14–19
- Howard C V and Reed M G 1998 *Unbiased stereology. Three-dimensional measurement in microscopy* (Royal Microscopy Society Microscopy Handbooks Series 41) (Oxford: BIOS Scientific)
- Ipiña S L and Ruiz-Marcos A 1986 Dendritic structure alterations induced by hypothyroidism in pyramidal neurons of the rat visual cortex *Dev. Brain Res.* **29** 61–7
- Ipiña S L, Ruiz-Marcos A, Escobar del Rey F and Morreale de Escobar G 1987 Pyramidal cortex cell morphology studied by multivariate analysis: effects of neonatal thyroidectomy, ageing and thyroxine substitution therapy *Dev. Brain Res.* **37** 219–29

- Jin X, Mathers P H, Szabo G, Katarova Z and Agmon A 2001 Vertical bias in dendritic trees of non-pyramidal neocortical neurons expressing GAD67-GFP in vitro *Cereb. Cortex* **11** 666–78
- Koenderink M J T H and Uylings H B M 1995 Postnatal maturation of layer V pyramidal neurons in the human prefrontal cortex. A quantitative Golgi analysis *Brain Res.* **678** 233–43
- Koenderink M J T H, Uylings H B M and Mrzljak L 1994 Postnatal maturation of the layer III pyramidal neurons in the human prefrontal cortex: a quantitative Golgi analysis *Brain Res.* **653** 173–82
- Kossel A, Löwel S and Bolz J 1995 Relationships between dendritic fields and functional architecture in striate cortex of normal and visually deprived cats *J. Neurosci.* **15** 3913–26
- Kötter R, Stephan K E, Palomero-Gallagher N, Geyer S, Schleicher A and Zilles K 2001 Multimodal characterisation of cortical areas by multivariate analyses of receptor binding and connectivity data *Anat. Embryol.* **204** 333–50
- Leontovich T A 1973 Methodik zur quantitativen Beschreibung subcorticaler Neurone *J. Hirnforsch.* **14** 59–87
- Leventhal A G and Schall J D 1983 Structural basis of orientation sensitivity of cat retinal ganglion cells *J. Comp. Neurol.* **220** 465–75
- MacDonald N 1983 *Trees and Networks in Biological Models* (Chichester: Wiley)
- McMullen N T, Glaser E M and Tagamets M 1984 Morphometry of spine-free nonpyramidal neurons in rabbit auditory cortex *J. Comp. Neurol.* **222** 383–95
- McMullen N T, Goldberger B, Suter C M and Glaser E M 1988 Neonatal deafening alters non-pyramidal dendrite orientation in auditory cortex: a computer microscope study in the rabbit *J. Comp. Neurol.* **267** 92–106
- Mungai J M 1967 Dendritic patterns in the somatic sensory cortex of the cat *J. Anat.* **101** 403–18
- O'Hanlon G M and Lowrie M B 1996 The effects of neonatal dorsal root section on the survival and dendritic development of lumbar motoneurons in the rat *Eur. J. Neurosci.* **8** 1072–7
- Parnavelas J G and Uylings H B M 1980 The growth of non-pyramidal neurons in the visual cortex of the rat: a morphometric study *Brain Res.* **193** 373–82
- Pearson J C, Norris J R and Phelps C H 1985 Subclassification of neurons in the subthalamic nucleus of the lesser bushbaby *Galago selegalensis*: a quantitative Golgi study using principle component analysis *J. Comp. Neurol.* **238** 323–39
- Rall W 1977 Core conductor theory and cable properties of neurons *Handbook of Physiology, section I: The Nervous System* ed J M Brookhart, V B Mountcastle and E R Kandel (Bethesda, MD: American Physiological Society) pp 39–97
- Ramakers G J, Avci B, van Hulst P, van Ooyen A, van Pelt J, Pool C W and Lequin M B 2001 The role of calcium signaling in early axonal and dendritic morphogenesis of rat cerebral cortex neurons under non-stimulated growth conditions *Dev. Brain Res.* **126** 163–72
- Rauschecker J P 1997 Mechanisms of compensatory plasticity in the cerebral cortex *Brain Plasticity* ed H J Freund, B A Sabel and O W Witte (Philadelphia, PA: Lippincott-Raven) pp 137–46
- Rauschecker J P 1997 Mechanisms of compensatory plasticity in the cerebral cortex *Adv. Neurol.* **73** 137–46
- Roberts N and Cruz-Orive L M 1993 Spatial distribution of curve length: concept and estimation *J. Microsc.* **173** 23–9
- Ruiz-Marcos A and Ipiña S L 1986 Hypothyroidism affects preferentially the dendritic densities on the more superficial region of pyramidal neurons of the rat cerebral cortex *Brain Res.* **393** 259–62
- Ruiz-Marcos A and Valverde F 1970 Dynamic architecture of the visual cortex *Brain Res.* **19** 25–39
- Ruiz-Marcos A 1983 Mathematical models of cortical structures and their application to the study of pathological conditions *Ramon y Cajal's Contribution to the Neurosciences* ed S Grisolia, C Guerri, F Samson, S Norton and F Reinoso-Suarez (Amsterdam: Elsevier) pp 209–22
- Ruiz-Marcos A, Cartagena Abella P, Garcia Garcia A, Escobar del Rey F and Morreale de Escobar G 1988 Rapid effects of adult-onset hypothyroidism on dendritic spines of pyramidal cells of the rat cerebral cortex *Exp. Brain Res.* **73** 583–8
- Sadler M and Berry M 1983 Morphometric study of the development of Purkinje cell dendritic trees in the mouse using vertex analysis *J. Microsc.* **131** 341–54
- Sadler M and Berry M 1988 Link-vertex analysis of Purkinje cell dendritic trees from the murine cerebellum *Brain Res.* **474** 130–46
- Schall J D and Leventhal A G 1987 Relationships between ganglion cell dendritic structure and retinal topography in the cat *J. Comp. Neurol.* **257** 149–59
- Schleicher A, Amunts K, Geyer S, Kowalski T, Schormann T, Palomero-Gallagher N and Zilles K 2000 A stereological approach to human cortical architecture: identification and delineation of cortical areas *J. Chem. Neuroanat.* **20** 31–47
- Segev I, Friedman A, White E L and Gutnick M J 1995 Electrical consequences of spine dimensions in a model of a cortical spiny stellate cell completely reconstructed from serial thin sections *J. Comput. Neurosci.* **2** 117–30
- Shepherd G M 1996 The dendritic spine: a multifunctional integrative unit *J. Neurophysiol.* **75** 2197–210

- Sholl D A 1953 Dendritic organization in the neurons of the visual and motor cortices of the cat *J. Anat.* **87** 387–406
- Smit G J, Uylings H B M and Veldmaat-Wansink L 1972 The branching pattern in dendrites of cortical neurons *Acta Morphol. Neerl.-Scand.* **9** 253–74
- Smit G J and Uylings H B M 1975 The morphometry of the branching pattern in dendrites of the visual cortex pyramidal cells *Brain Res.* **87** 41–53
- Stevens C F and Van den Pol A N 1982 Appendix to Van den Pol and Cassidy (1982)
- Trommald M, Jensen V and Andersen P 1995 Analysis of dendritic spines in rat CA1 pyramidal cells intracellularly filled with a fluorescent dye *J. Comp. Neurol.* **353** 260–74
- Uylings H B M and Smit G J 1975 Three-dimensional branching structure of pyramidal cell dendrites *Brain Res.* **87** 55–60
- Uylings H B M, Smit G J and Veltman W A M 1975 Ordering methods in quantitative analysis of branching structures of dendritic trees *Physiology and Pathology of Dendrites, Advances in Neurology* ed G W Kreutzberg (New York: Raven) pp 47–254
- Uylings H B M and Veltman G J 1975 Characterizing a dendritic bifurcation *Neurosci. Lett.* **1** 128–30
- Uylings H B M, Kuypers K, Diamond M C and Veltman W A M 1978a Effects of differential environment on plasticity of dendrites of cortical pyramidal neurons in adult rats *Exp. Neurol.* **62** 658–77
- Uylings H B M, Kuypers K and Veltman W A M 1978b Environmental influences on neocortex in later life *Maturation of the Nervous System. Progress in Brain Research* ed M A Corner, R E Baker, N E van de Poll, D F Swaab and H B M Uylings (Amsterdam: Elsevier) pp 261–74
- Uylings H B M, Van Eden C G and Hofman M A 1986a Morphometry of size/volume variables and comparison of their bivariate relations in the nervous system under different conditions *J. Neurosci. Methods* **18** 19–37
- Uylings H B M, Ruiz-Marcos A and Van Pelt J 1986b The metric analysis of the three-dimensional dendritic tree patterns: a methodological review *Special Issue Morphometry and Stereology in Neurosciences J. Neurosci. Methods* **18** 127–51
- Uylings H B M, Van Pelt J and Verwer R W H 1989a Topological analysis of individual neurons *Computer Techniques in Neuroanatomy* ed J J Capowski (New York: Plenum) pp 215–39
- Uylings H B M, Van Pelt J, Verwer R W H and McConnell P 1989b Statistical analysis of neuronal populations *Computer Techniques in Neuroanatomy* ed J J Capowski (New York: Plenum) pp 241–64
- Uylings H B M, Van Pelt J, Parnavelas J G and Ruiz-Marcos A 1994 Geometrical and topological characteristics in the dendritic development of cortical pyramidal and nonpyramidal neurons *The Self-Organizing Brain: from Growth Cones to Functional Networks (Prog. Brain Res., vol 102)* (Amsterdam: Elsevier) pp 109–23
- Uylings H B M, West J M, Coleman P D, De Brabander J M and Flood D G 2000 Neuronal and cellular changes in ageing brain *Neurodegenerative Dementias. Clinical Features and Pathological Mechanisms* ed C Clark and J Trojanowski (New York: McGraw-Hill) pp 61–76
- Valverde F 1970 The Golgi method. A tool for comparative structural analyses *Contemporary Research Methods in Neuroanatomy* ed W J H Nauta and S O E Ebbeson (Berlin: Springer) pp 12–31
- Van den Pol A N and Cassidy J R 1982 The hypothalamic arcuate nucleus of the rat: a quantitative Golgi analysis *J. Comp. Neurol.* **204** 65–98
- Van der Loos H 1959 Dendro-dendritic connections in the cerebral cortex *Doctoral Dissertation* University of Amsterdam, H Stam p 99 (in Dutch)
- Van Ooyen A 1994 Activity-dependent neural network development *Network: Comput. Neural Syst.* **5** 401–23
- Van Ooyen A, Duijnhouwer J, Remme M W H and Van Pelt J 2002 The effect of dendritic topology on firing patterns in model neurons *Network: Comput. Neural Syst.* **13** 311–25 (this issue)
- Van Pelt J and Verwer R W H 1983 The exact probabilities of branching patterns under terminal and segmental growth hypotheses *Bull. Math. Biol.* **45** 269–85
- Van Pelt J and Verwer R W H 1984 New classification methods of branching patterns *J. Microsc.* **136** 23–4
- Van Pelt J, Uylings H B M and Verwer R W H 1989 Distributional properties of measures of tree topology *Acta Stereol.* **8** 465–70
- Van Pelt J and Uylings H B M 1999 Modeling the natural variability in the shape of dendritic trees: application to basal dendrites of small rat cortical layer 5 pyramidal neurons *Neurocomputing* **26–7** 305–11
- Van Pelt J, Dityatev A E and Uylings H B M 1997 Natural variability in the number of dendritic segments: model-based inferences about branching during neurite outgrowth *J. Comp. Neurol.* **387** 325–40
- Van Pelt J, Uylings H B M, Verwer R W H, Pentney R J and Woldenberg M J 1992 Tree asymmetry—a sensitive and practical measure for binary topological trees *Bull. Math. Biol.* **54** 759–84
- Van Pelt J, Van Ooyen A and Uylings H B M 2001a Modelling dendritic geometry and the development of nerve connections *Computational Neuroscience. Realistic Modeling for Experimentalists* ed E De Schutter (Boca Raton, FL: CRC Press) pp 179–208

- Van Pelt J, Van Ooyen A and Uylings H B M 2001b The need for integrating neuronal morphology databases and computational environments in exploring neuronal structure and function *Anat. Embryol.* **204** 255–65
- Van Pelt J and Uylings H B M 2002 Branching rates and growth functions in the outgrowth of dendritic branching patterns *Network: Comput. Neural Syst.* **13** 261–81 (this issue)
- Van Veen M and van Pelt J 1992 A model for outgrowth of branching neuritis *J. Theor. Biol.* **159** 1–23
- Verwer R W H, Van Pelt J and Uylings H B M 1992 An introduction to topological analysis of neurones *Quantitative Methods in Neuroanatomy* ed M G Stewart (New York: Wiley) pp 295–323
- Ward R, Moreau B, Marchand M J and Garenc C 1995 A note on the distribution of dendritic spines *J. Brain Res.* **36** 519–22
- White E L and Rock M P 1980 Three-dimensional aspects and synaptic relationships of a Golgi-impregnated spiny stellate cell reconstructed from serial thin sections *J. Neurocytol.* **9** 615–36
- Williams R S and Matthijsse S 1986 Morphometric analysis of granule cell dendrites in the mouse dentate gyrus *J. Comp. Neurol.* **215** 154–64
- Wolf E, Birinyi A and Pomahazi S 1995 A fast 3-dimensional neuronal tree reconstruction system that uses cubic polynomials to estimate dendritic curvature *J. Neurosci. Methods* **63** 137–45
- Woolley C S 1999 Structural plasticity of dendrites *Dendrites* ed G Stewart, N Pruston and M Häusser (New York: Oxford University Press) pp 339–64
- Yelnik J, Percheron G, Francois C and Burnod Y 1983 Principal component analysis: a suitable method for the 3-dimensional study of the shape, dimensions and orientation of dendritic arborizations *J. Neurosci. Methods* **9** 115–25